

## Synthesis and Characterization of Mn, Ce Co-Doped CdS Nanoparticles Synthesized Via Co-Precipitation Method

M. Sreenivas<sup>1</sup>, G. S. Harish<sup>2</sup>, P. Sreedhara Reddy<sup>3</sup>

<sup>1,2,3</sup>Department of Physics, Sri Venkateswara University, Tirupati, Andhra Pradesh-517502, India

**Abstract:** Mn, Ce co-doped CdS nanoparticles were prepared by chemical co-precipitation method at room temperature. The prepared samples were characterized by X-ray diffraction (XRD), scanning electron microscopy (SEM), energy dispersive analysis of X-rays (EDAX), photoluminescence (PL) and high resolution Raman spectroscopic techniques. X-ray diffraction studies showed that the diameter of the particles was around 10-12 nm. Broadened XRD peaks revealed the formation of nanoparticles with wurtzite structure. The Raman spectra of undoped and Mn, Ce ions co-doped CdS nanoparticles showed longitudinal optical mode. Compared with the 1LO and 2LO Raman modes (296 and 590  $\text{cm}^{-1}$ ) of undoped CdS nanoparticles, the Raman modes of Mn, Ce co-doped CdS nanoparticles were slightly shifted towards lower frequency. PL spectra of the samples showed remarkable enhancement in the intensity upon doping.

**Keywords:** Chemical synthesis, Nanoparticles, Photoluminescence, Raman spectra, XRD

### I. INTRODUCTION

The Nanomaterials doped with optically active luminescence centers create new opportunities for luminescence research and also for the application of nanometer-scale structured materials. Doped II–VI semiconductors like ZnS:Cu, CdS:Mn, etc have been intensively investigated with new luminescence centers [1–3]. Cadmium sulfide is an important semiconducting material that has attracted much interest owing to their unique electronic and optical properties, and their potential applications in solar energy conversion, photoconducting cells, non-linear optics and heterogeneous photocatalysis [4, 5]. The extended life time of charge carriers as observed in Mn doped CdS, for example, could be advantageous to improve the performance of solar energy conversion systems. When doping with Mn, for example, the photoinduced electrons in the conduction band of CdS are transferred to the Mn  $^4T_1$  state, which temporarily traps the electrons and prevents recombination with holes or oxidized electrolyte species [7]. Mn<sup>2+</sup> doped CdS NPs are interesting because of the fact that Mn<sup>2+</sup> ions provide good traps for the excited electrons, which give rise to their potential use in nonlinear optics, electronic and optoelectronic devices [8-10]. Many literatures from different groups have reported the optical properties of various doped nanocrystals and the potential application of these luminescent materials. Today, various transition metal ions and rare-earth ions as impurities doped in CdS nanocrystalline materials have many interesting optical properties [11-15].

Previous works have shown that large quantities of nanomaterials were prepared by various methods artificially. Optoelectronic properties, particle sizes, and morphologies of nanomaterials have a close relation to preparation conditions. Appropriate preparation methods should be utilized according to the demands for different applications. Nanocrystalline CdS, CdTe, CdSe, ZnSe and PbS have been synthesized by a variety of methods including precipitation, sputtering, electrochemical deposition and inverse micelles. A reduction in the particle size strongly influences the crystallinity, melting point and structural stability. In the present work, Ce and Mn co-doped CdS nanoparticles were prepared via cost effective, facile chemical co-precipitation method at room temperature and the structural, morphological, chemical composition and luminescent properties of these nanoparticles were investigated.

### II. EXPERIMENTAL

All the chemicals used were of analytical reagent grade and used without further purification. Undoped CdS, cerium (Ce) (2 at.%) and manganese (Mn) (0, 2, 4 and 6 at.%) co-doped CdS nanoparticles were prepared by a simple chemical co-precipitation method with biocompatible polyvinylpyrrolidone (PVP) as a capping agent. The reactants were CdCl<sub>2</sub>, CeCl<sub>3</sub>.7H<sub>2</sub>O (2at. %), MnSO<sub>4</sub>.H<sub>2</sub>O, Na<sub>2</sub>S and polyvinylpyrrolidone (PVP). Ultrapure de-ionized water was used as the reaction medium in all the synthesis steps. In a typical

synthesis, desired molar proportions of CdCl<sub>2</sub>, CeCl<sub>3</sub>.7H<sub>2</sub>O (2at.%) and MnSO<sub>4</sub>.H<sub>2</sub>O (0,2,4 and 6 at.%) each in 50 ml were dissolved in ultrapure de-ionized water. An appropriate amount of capping agent PVP was added to control the growth of the nanoparticles during the reaction. Later stirring the solution for 60 min, Na<sub>2</sub>S solution was drop wisely added to the solution at room temperature under constant stirring which was continued for four hours to get fine precipitation. The obtained precipitate was washed with de-ionized water several times. Finally, the powders were vacuum dried for 3 hours at 80 °C to obtain Ce, Mn co-doped CdS nanoparticles. Undoped CdS nanoparticles were synthesized by the same procedure.

### III. CHARACTERIZATION

The as synthesized nanopowders were characterized by studying the structure, composition, surface morphology and optical properties. The X-ray diffraction patterns of the samples were collected on a Rigaku D X-ray diffractometer using Cu-K $\alpha$  radiation ( $\lambda=1.5406\text{\AA}$ ). The morphology and elemental composition of the prepared samples were analyzed through EDAX using Oxford Inca Penta FeTX3 EDS instrument attached to a Carl Zeiss EVO MA 15 scanning electron microscope. Photoluminescence spectra was recorded in the wavelength range of 400–650 nm using a PTI (Photon Technology International) Fluorimeter with a Xe-arc lamp of power 60 W and an excitation wavelength of 320 nm. Raman Spectroscopic studies of the as prepared samples were carried out using a LabRam HR800 Raman Spectrometer.

### IV. RESULTS AND DISCUSSION

#### 4.1. Structural Analysis

Fig. 1 represents the XRD patterns of undoped CdS and Ce, Mn co-doped CdS nanoparticles. The broadening of peaks indicates that particles are in the nanosize regime. The XRD pattern shows (100), (002), (101), (102), (110), (103) and (112) planes of wurtzite CdS corresponding to JCPDS File No. 41-1049. The planes (110), (103) and (112) clearly distinguish the wurtzite structure of the Mn doped CdS NPs. The intensity of the plane (102) is very low and this intensity increases as the doping concentration of Mn<sup>2+</sup> increases. The increased intensity of the plane (102) in doped CdS may be due to increased crystallinity in this plane on doping [16]. The low intensity in undoped system may be due to imperfection or due to the strain or low crystallinity in the crystals [16]. In the diffraction patterns, peak broadening is due to four factors: deformation of the lattice, crystalline domain size, crystalline faults and domain size distribution [16]. From the XRD spectra it was also observed that no diffraction peaks corresponding to the impurity phases were detected and this rule out Ce or Mn precipitation or secondary phases. The average particle size calculated by Debye Scherrer's equation [a] for Ce, Mn co-doped CdS nanoparticles lies in the range of 10-12 nm.

$$D = \frac{0.94\lambda}{\beta_{hkl} \cos \theta} \text{----- [a]}$$

Where, D is the average particle size and  $\beta_{hkl}$  is full width at half maximum of the XRD peak expressed in radians and  $\theta$  is the position of the diffraction peak. The average particle size of the samples was calculated by Debye Scherrer's equation [a].

#### 4.2. Morphological and Compositional Analysis

Fig. 2 shows the morphology of Ce, Mn co-doped CdS nanoparticles. Figures 2(a), 2(b), 2(c), 2(d) and 2(e) show the SEM images of pure CdS, CdS: Ce<sub>x</sub>, Mn<sub>y</sub> (x=2%, y=0%, 2% and 4%, 6%) respectively. SEM images showed the agglomerated nanoparticles of the prepared samples.

The chemical composition analysis of the Ce, Mn co-doped CdS nanoparticles was done using the EDAX technique. The EDAX spectra of the CdS: Ce, Mn nanoparticles shown in Fig. 3 confirms the effective doping of Ce and Mn. Figures 3(a), 3(b), 3(c), 3(d) and 3(e) shows the EDAX spectra of pure CdS, CdS: Ce<sub>x</sub>, Mn<sub>y</sub> (x=2%, y= 0%, 2%, 4%, 6%) respectively, confirmed that the samples were composed of Cd, Ce, Mn and S elements in desired composition and without any impurities.

#### 4.3. Photoluminescence Studies

Fig. 4 shows the PL spectra recorded at room temperature with an excitation wavelength of 390 nm for pure CdS, Ce (2%) and Mn (0, 2, 4 and 6 at. %) co-doped CdS nanoparticles. High intense peaks centered at 450 nm are assigned to band edge emission of CdS nanocrystallites. The peaks of the CdS nanocrystallites doped with Ce<sup>3+</sup> ions were almost the same as those of the pure CdS nanocrystallites. However, the fluorescence intensity of the CdS nanocrystallites doped with Ce<sup>3+</sup> ions is about 6 times of that of CdS

nanoparticles. The broad peak located around 605 nm may be arises from sulphur sites and the  $Mn^{2+}$  luminescence is caused by emission from the first excited state  ${}^4T_1$  to the ground state  ${}^6A_1$  [17-18]. An additional red-shifted emission feature is observed with increase in  $Mn^{2+}$  concentration.  $Mn^{2+}$  pairing has also been observed in  $Zn_2SiO_4:Mn^{2+}$  [19]. There are however a few reports on  $Mn^{2+}$  pairing in CdS: Mn nanoparticles and Chory et al.[20] were the only group reporting a red (640 nm) luminescence from CdS: Mn nanoparticles. Present studies show that, the enhanced luminescence properties of the PVP capped CdS: Ce, Mn nanoparticles that continued upto Mn (4 at.%) and a decrease in luminescence is observed at Mn (6 at.%). The red luminescence is attributed to  $Mn^{2+}$  pairing effect due to high concentration of  $Mn^{2+}$  and  $Ce^{3+}$  in CdS host lattice.

#### 4.4. Raman Spectroscopy

Raman spectra of the undoped and Ce (2 at. %) and Mn (0, 2, 4 and 6 at. %) co-doped CdS nanoparticles in the frequency range 200 - 700  $cm^{-1}$  are shown in Fig. 5. The Raman spectrum of bulk CdS exhibits the first longitudinal optical phonons (1LO) peak at 304  $cm^{-1}$  and the second longitudinal optical phonons (2LO) peak at 600  $cm^{-1}$ [21]. The Raman spectrum of undoped CdS nanoparticles exhibited strong but broad peaks at 296 and 590 $cm^{-1}$  corresponding to 1LO and 2LO optical phonons, respectively. The frequency shift of the Raman bands towards lower frequency could be due to large surface to volume ratio. In the case of large surface-to-volume ratio, surface scattering contributes more to the Raman signal than volume scattering. The frequency shifts of the 1LO and 2LO modes observed in the present samples may be attributed to a smaller size and larger surface-to-volume ratio compared with that of the undoped CdS. Another possible reason for the Raman shift is that the ionic radius of  $Ce^{3+}$  is higher than that of  $Cd^{2+}$ . Lattice defects are introduced or intrinsic host lattice defects are activated when  $Ce^{3+}$  and  $Mn^{2+}$  ions are incorporated. The  $Ce^{3+}$  and  $Mn^{2+}$  ions tend to occupy substitutional cationic sites resulting in host lattice defects. Further, no additional Raman modes due to Ce and Mn impurities were observed in Ce and Mn co-doped CdS nanoparticles. This revealed the absence of impurity phases in the prepared nanopowder samples.

#### V. FIGURES

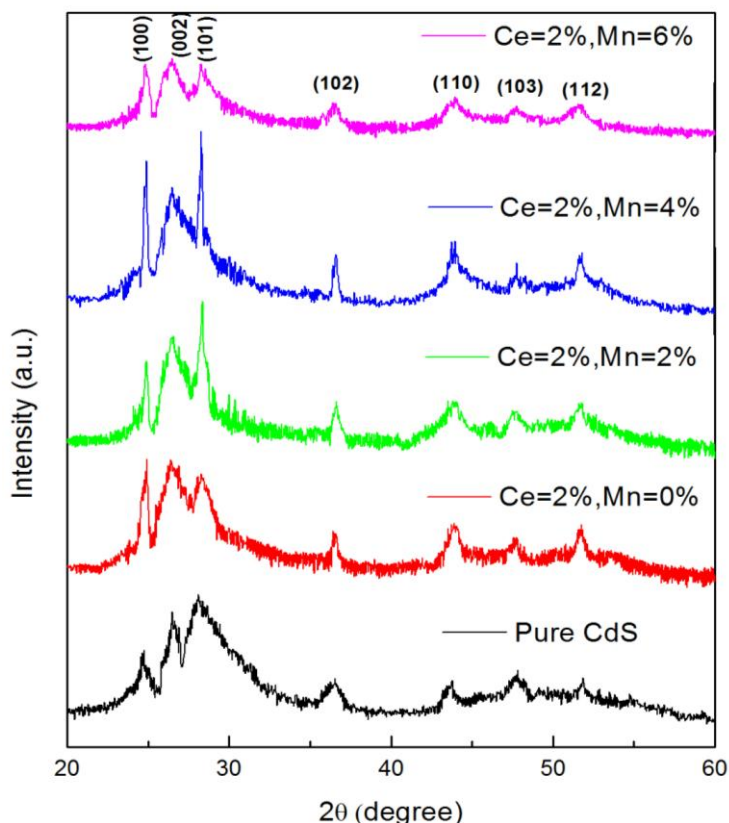
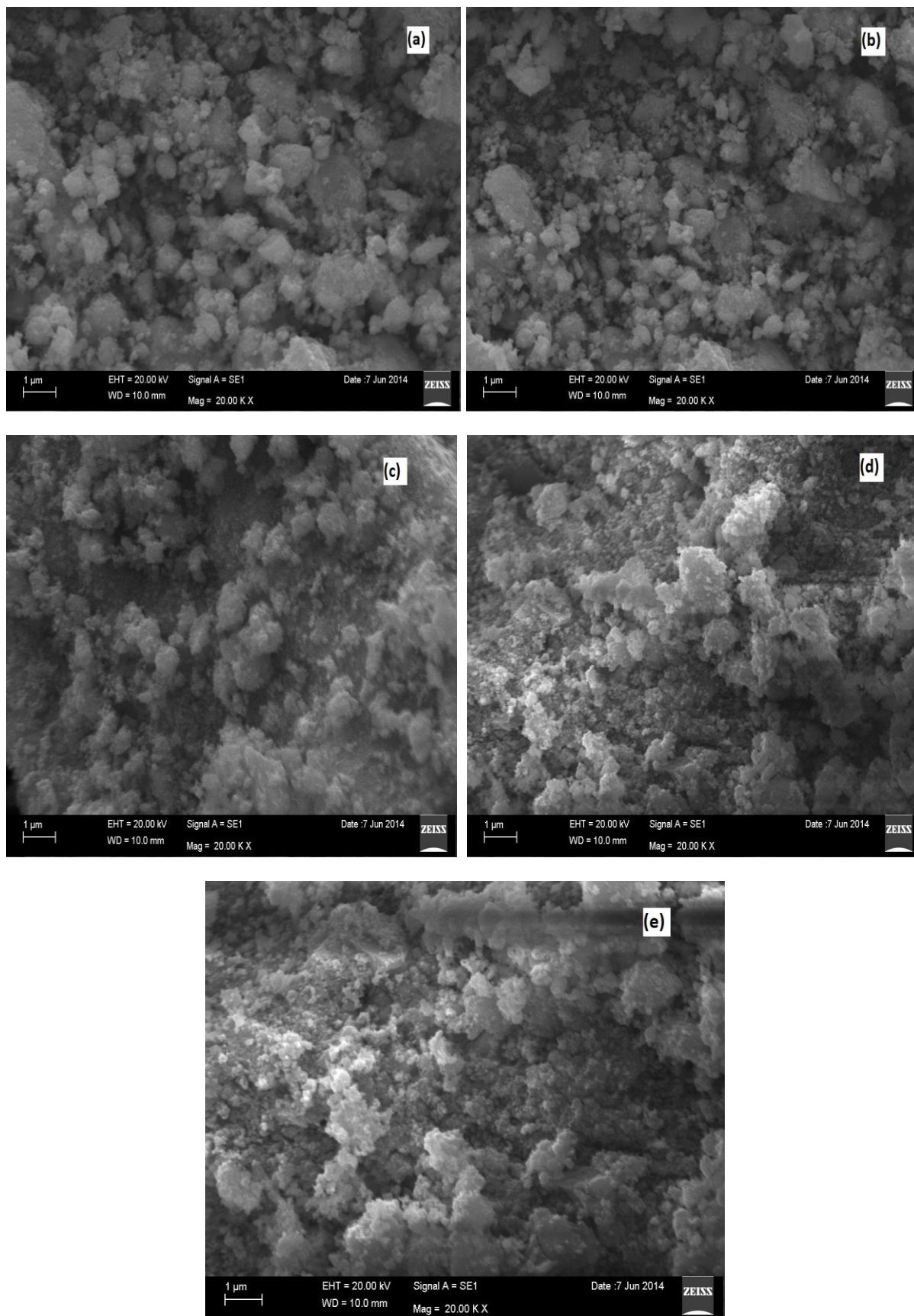


Fig.1. XRD patterns of undoped CdS and Ce, Mn co-doped CdS nanoparticles



**Fig. 2.** SEM images of CdS: Ce, Mn nanoparticles. (a) Pure CdS, (b) Ce=2%, Mn=0%, (c) Ce=2%, Mn=2%, (d) Ce=2%, Mn=4% and (e) Ce=2%, Mn=6%

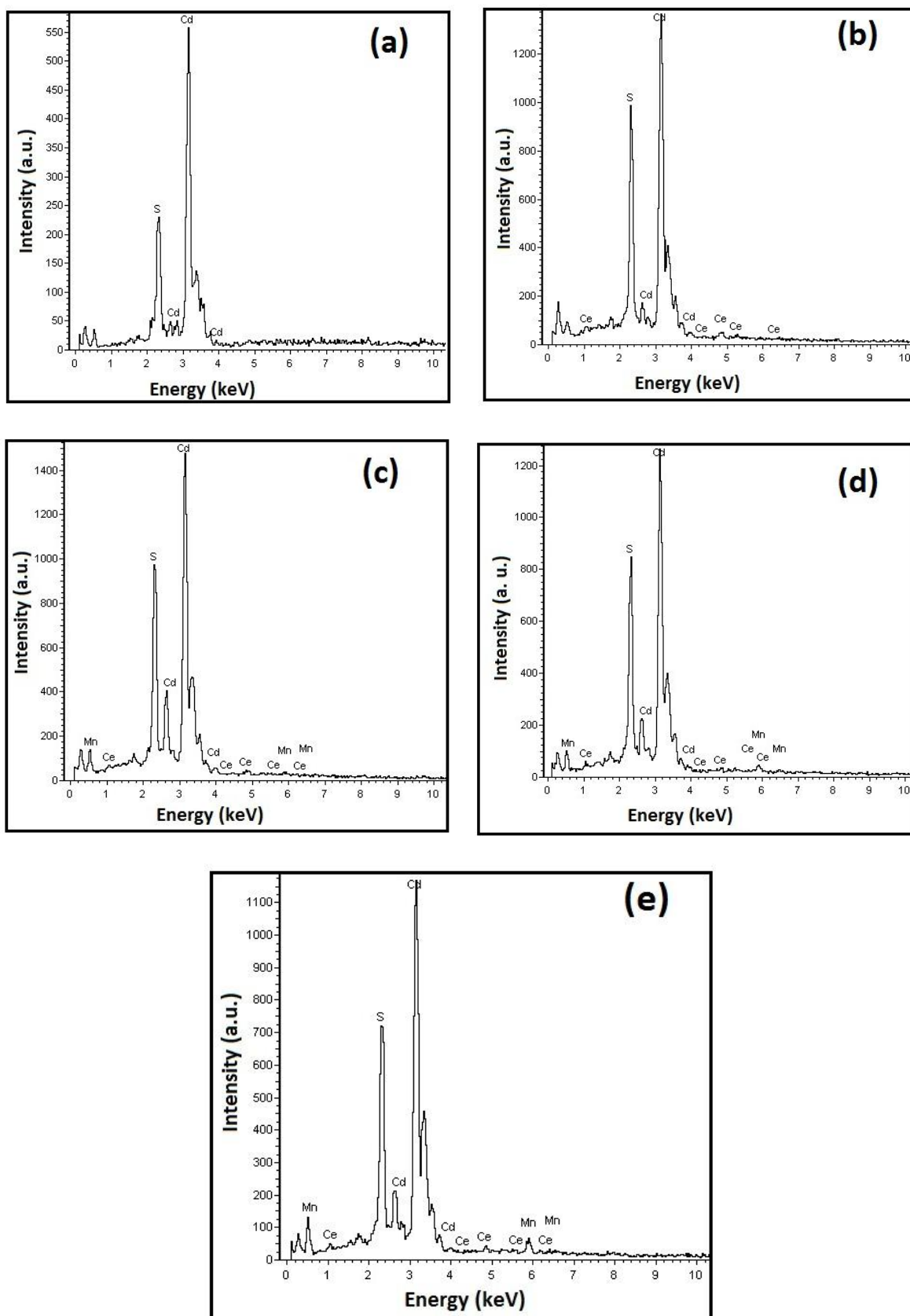


Fig. 3. Representative EDS spectrum of Ce, Mn co-doped CdS nanoparticles. (a) Pure CdS, (b) Ce=2%, Mn=0%, (c) Ce=2%, Mn=2%, (d) Ce=2%, Mn=4% and (e) Ce=2%, Mn=6%.

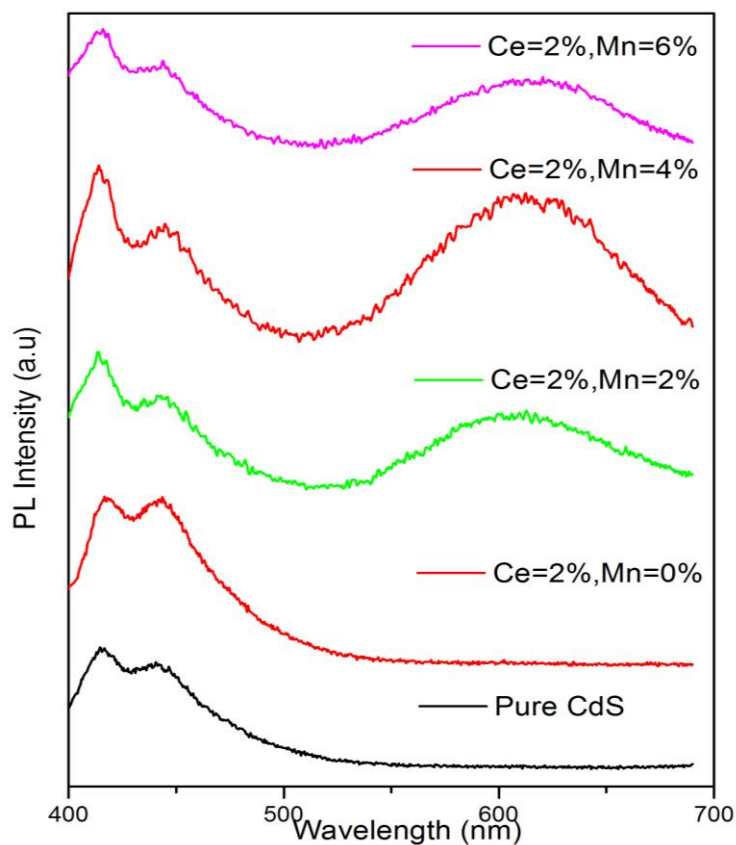


Fig. 4. Photoluminescence spectra of undoped and Ce, Mn co-doped CdS nanoparticles.

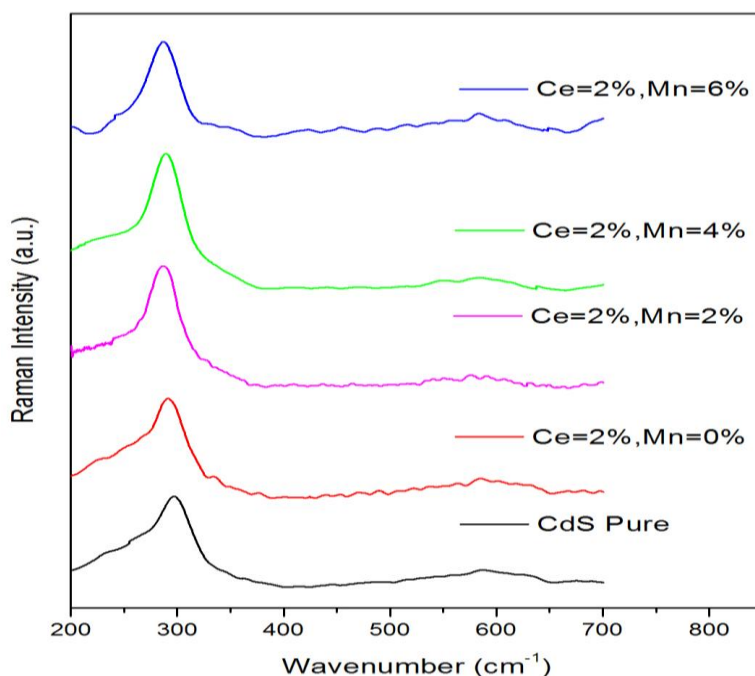


Fig. 5. Raman spectra of undoped CdS and Ce, Mn co-doped CdS nanoparticles

## VI. CONCLUSION

In summary, Ce and Mn co-doped CdS nanoparticles have been successfully synthesized by chemical co-precipitation method at room temperature. X-ray diffraction (XRD) measurements showed that the Ce, Mn co-doped CdS nanoparticles have a wurtzite structure. The morphology and composition of CdS: Ce, Mn

nanoparticles were successfully studied by scanning electron microscopy (SEM) and energy dispersive X-ray spectroscopy (EDAX) respectively. The luminescence peak of CdS nanoparticles is centered at 450 nm and is enhanced to 6 times by doping with Ce<sup>3+</sup> ions. The emission peaks of CdS: Ce, Mn nanoparticles are observed at 450 nm and broad emission peak around 610 nm are enhanced effectively that of undoped CdS nanoparticles with a red shift. Undoped CdS showed Raman peaks at 296 and 590 cm<sup>-1</sup> correspond to the 1LO mode and 2LO mode of the samples showed a slight red shift and asymmetric broadening indicating phonon confinement effects.

### Acknowledgements

One of the authors, Mr. G. S. Harish, is thankful to C.S.I.R., New Delhi, for awarding a Junior Research Fellowship.

### REFERENCES

- [1] W. Zhang, H.R. Lee, Synthesis and optical property of water-soluble ZnS:Cu quantum dots by use of thioglycolic acid, *Appl. Opt.* 49 (2010) 2566–2570.
- [2] A. Nag, S. Chakraborty, D.D. Sarma, To dope Mn<sup>2+</sup> in a semiconducting nanocrystal, *J. Am. Chem. Soc.* (2008) 10605–10611.
- [3] A. Nag, S. Sapra, C. Nagamani, A. Sharma, N. Pradhan, S.V. Bhat, D.D. Sarma, A study of Mn<sup>2+</sup> doping in CdS nanocrystals, *Chem. Mater.* 19 (2007) 3252–3259.
- [4] P. Verma, G.S. Manoj, A.C. Pandey, Organic capping-Effect and mechanism in Mn-doped CdS nanocomposites, *Physica B*, 405 (2010) 1253–1257.
- [5] G. Murugadoss, Synthesis of high quality and monodisperse CdS: Mn<sup>2+</sup>/ZnS and CdS:Mn<sup>2+</sup>/CdS core-shell nanoparticles, *Superlattices and Microstructures* 52 (2012) 1026–1042.
- [6] W. Lee, W.C. Kwak, S.K. Min, J.C. Lee, W. S. Chae, Y. M. Sung, S.H. Han, *Electrochem. Commun.* (2008) 1699–1702
- [7] M. Liu, Y. Du, L. Ma, D. Jing, L. Guo, Manganese doped cadmium sulfide nanocrystal for hydrogen production from water under visible light, *International Journal of Hydrogen Energy*, 37 (2012) 730-736
- [8] N.V. Hullavarad, S.S. Hullavarad, P.C. Karulkar, Review of Cadmium Sulfide CdS Nanotechnology: synthesis and Applications, *J. Nanosci. Nanotechnol.* 8 (2008) 3272-3299.
- [9] A. Nag, R. Cherian, P. Mahadevan, A.V. Gopal, A. Hazarika, A. Mohan, A. S. Vengurlekar, D. D. Sarma, Size-Dependent Tuning of Mn<sup>2+</sup> Emission in Mn<sup>2+</sup>-Doped CdS Nanocrystals: Bulk vs Surface, *J. Phys. Chem. C*, 114 (2010) 18323–18329.
- [10] M. A. White, A. L. Weaver, R. Beaulac, D. R. Gamelin, Electrochemically Controlled Auger Quenching of Mn<sup>2+</sup> Photoluminescence in Doped Semiconductor Nanocrystals, *ACS NANO*, 5, 5 (2011) 4158-4168.
- [11] S. Salimian, S.F. Shayesteh, Structural, Optical and Magnetic Properties of Mn-doped CdS diluted Magnetic Semiconductor Nanoparticles, *J Supercond Nov Magn.* 25 (2012) 2009–2014.
- [12] R. Xie, U. Kolb, J. Li, T. Basche, A. Mews, Synthesis and characterization of highly luminescent CdSe-core CdS/Zn0.5Cd0.5S/ZnS multishell nanocrystals, *J. Am. Chem. Soc.* 127 (2005) 7480–7488.
- [13] M. Amelia, R. Flamini, L. Latterini, Recovery of CdS nanocrystal defects through conjugation with proteins, *Langmuir* 26 (2010) 10129–10134.
- [14] H. Zhao, E.P. Douglas, Preparation of corona-embedded CdS nanoparticles, *Chem. Mater.* 14 (2002) 1418–1423.
- [15] Y. Yang, O. Chen, A. Angerhofer, Y.C. Cao, Radial-position controlled doping in CdS/ZnS core/shell nanocrystals, *J. Am. Chem. Soc.* (2006) 12428–12429.
- [16] B.D. Cullity, S.R. Stock, *Elementary of X-ray Diffraction*, 3<sup>rd</sup> ed., Prentice-Hall, Englewood Cliffs, NJ, 2001 Y. Wang, N. Herron, *J. Phys. Chem.* 95 (1991) 525-532.
- [17] C. Cheng, G. Xu, H. Zhang, H. Wang, J. Cao, H. Ji, Solvothermal synthesis and photoluminescence properties of single-crystal Mn<sup>2+</sup> doped CdS nanowires, *Materials Chemistry and Physics* 97 (2006) 448–451.
- [18] S. Liu, F. Liu, H. Guo, Z. Zhang, Z. Wang, Surface states induced photoluminescence from Mn<sup>2+</sup> doped CdS nanoparticles, *Solid State Communications* 115 (2000) 615–618.
- [19] N. Taghavinia, G. Lerondel, H. Makino, A. Parisini, A. Yamamoto, T. Yao, Y. Kawazoe, T. Goto, Structural and Optical Properties of Oxidized Porous Silicon Layers Activated by Zn<sub>2</sub>SiO<sub>4</sub> : Mn<sup>2+</sup>, *J. Electrochem. Soc.* 149 (2002) G251-G256.
- [20] C.B. Chory, C. Remenyi, C. Dem, M. Schmitt, W. Kiefer, C. Gould, C. Ruster, G. Schmidt, D.M. Hofmann, D. Pfistererd, G. Muller, Synthesis and characterization of manganese-doped CdS nanoparticles, *Phys. Chem. Chem. Phys.* 5 (2003) 1639-1643.
- [21] A.K. Gupta, R. Kripal, EPR and photoluminescence properties of Mn<sup>2+</sup> doped CdS nanoparticles synthesized via co-precipitation method, *Spectrochimica Acta Part A: Molecular and Biomolecular Spectroscopy* 96 (2012) 626–631.